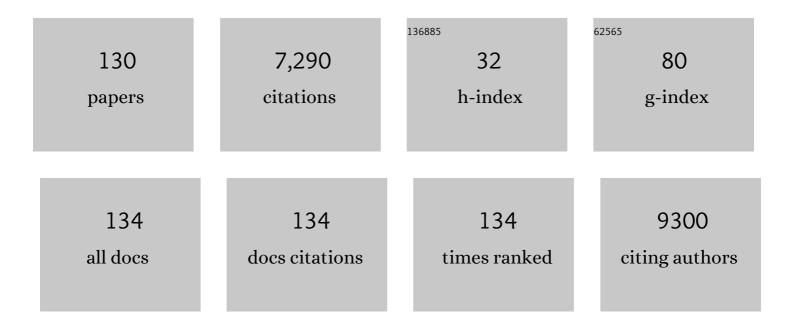
List of Publications by Year in descending order

Source: https://exaly.com/author-pdf/7013800/publications.pdf Version: 2024-02-01



#	Article	IF	CITATIONS
1	Arterial spin labeling MR image denoising and reconstruction using unsupervised deep learning. NMR in Biomedicine, 2022, 35, e4224.	1.6	13
2	Penalized-Likelihood PET Image Reconstruction Using 3D Structural Convolutional Sparse Coding. IEEE Transactions on Biomedical Engineering, 2022, 69, 4-14.	2.5	15
3	Direct Reconstruction of Linear Parametric Images From Dynamic PET Using Nonlocal Deep Image Prior. IEEE Transactions on Medical Imaging, 2022, 41, 680-689.	5.4	21
4	Nuclear Medicine and Artificial Intelligence: Best Practices for Algorithm Development. Journal of Nuclear Medicine, 2022, 63, 500-510.	2.8	43
5	Artificial intelligence for stepwise diagnosis and monitoring of COVID-19. European Radiology, 2022, 32, 2235-2245.	2.3	22
6	Deep Learning-Based Four-Region Lung Segmentation in Chest Radiography for COVID-19 Diagnosis. Diagnostics, 2022, 12, 101.	1.3	12
7	A Review of Deep Learning Methods for Compressed Sensing Image Reconstruction and Its Medical Applications. Electronics (Switzerland), 2022, 11, 586.	1.8	13
8	Risk assessment for acute kidney injury and death among new COVID-19 positive adult patients without chronic kidney disease: retrospective cohort study among three US hospitals. BMJ Open, 2022, 12, e053635.	0.8	1
9	End-to-end deep learning for interior tomography with low-dose x-ray CT. Physics in Medicine and Biology, 2022, 67, 115001.	1.6	8
10	Connectivity-based Cortical Parcellation via Contrastive Learning on Spatial-Graph Convolution. BME Frontiers, 2022, 2022, .	2.2	1
11	Ms-Gwnn: Multi-Scale Graph Wavelet Neural Network for Breast Cancer Diagnosis. , 2022, , .		4
12	Joint Attention for Medical Image Segmentation. , 2022, , .		0
13	Unsupervised PET logan parametric image estimation using conditional deep image prior. Medical Image Analysis, 2022, 80, 102519.	7.0	6
14	MR-Based Attenuation Correction for Brain PET Using 3-D Cycle-Consistent Adversarial Network. IEEE Transactions on Radiation and Plasma Medical Sciences, 2021, 5, 185-192.	2.7	22
15	Attenuation correction using deep Learning and integrated UTE/multi-echo Dixon sequence: evaluation in amyloid and tau PET imaging. European Journal of Nuclear Medicine and Molecular Imaging, 2021, 48, 1351-1361.	3.3	14
16	A Graph Gaussian Embedding Method for Predicting Alzheimer's Disease Progression With MEG Brain Networks. IEEE Transactions on Biomedical Engineering, 2021, 68, 1579-1588.	2.5	19
17	Deep metric learning-based image retrieval system for chest radiograph and its clinical applications in COVID-19. Medical Image Analysis, 2021, 70, 101993.	7.0	46
18	Self-Supervised Dynamic CT Perfusion Image Denoising With Deep Neural Networks. IEEE Transactions on Radiation and Plasma Medical Sciences, 2021, 5, 350-361.	2.7	32

#	Article	IF	CITATIONS
19	Characterization of Brain Iron Deposition Pattern and Its Association With Genetic Risk Factor in Alzheimer's Disease Using Susceptibility-Weighted Imaging. Frontiers in Human Neuroscience, 2021, 15, 654381.	1.0	8
20	A multi-center study of COVID-19 patient prognosis using deep learning-based CT image analysis and electronic health records. European Journal of Radiology, 2021, 139, 109583.	1.2	26
21	Iterative material decomposition for spectral CT using self-supervised Noise2Noise prior. Physics in Medicine and Biology, 2021, 66, 155013.	1.6	17
22	Populational and individual information based PET image denoising using conditional unsupervised learning. Physics in Medicine and Biology, 2021, 66, 155001.	1.6	15
23	Left Ventricle Quantification Challenge: A Comprehensive Comparison and Evaluation of Segmentation and Regression for Mid-Ventricular Short-Axis Cardiac MR Data. IEEE Journal of Biomedical and Health Informatics, 2021, 25, 3541-3553.	3.9	8
24	Federated learning for predicting clinical outcomes in patients with COVID-19. Nature Medicine, 2021, 27, 1735-1743.	15.2	300
25	The Evolution of Image Reconstruction in PET. PET Clinics, 2021, 16, 533-542.	1.5	20
26	Rapid high-quality PET Patlak parametric image generation based on direct reconstruction and temporal nonlocal neural network. NeuroImage, 2021, 240, 118380.	2.1	8
27	Lowâ€dose CT reconstruction with Noise2Noise network and testingâ€ŧime fineâ€ŧuning. Medical Physics, 2021, 48, 7657-7672.	1.6	21
28	Classification of Exacerbation Frequency in the COPDGene Cohort Using Deep Learning With Deep Belief Networks. IEEE Journal of Biomedical and Health Informatics, 2020, 24, 1805-1813.	3.9	24
29	Four-Dimensional Modeling of fMRI Data via Spatio–Temporal Convolutional Neural Networks (ST-CNNs). IEEE Transactions on Cognitive and Developmental Systems, 2020, 12, 451-460.	2.6	28
30	Automated Semantic Segmentation of Red Blood Cells for Sickle Cell Disease. IEEE Journal of Biomedical and Health Informatics, 2020, 24, 3095-3102.	3.9	29
31	Severity and Consolidation Quantification of COVID-19 From CT Images Using Deep Learning Based on Hybrid Weak Labels. IEEE Journal of Biomedical and Health Informatics, 2020, 24, 3529-3538.	3.9	31
32	A new Graph Gaussian embedding method for analyzing the effects of cognitive training. PLoS Computational Biology, 2020, 16, e1008186.	1.5	16
33	A new stochastic graph embedding method for Alzheimer's disease earlyâ€stage prediction and intervention evaluation. Alzheimer's and Dementia, 2020, 16, e047329.	0.4	0
34	Penalized Parametric PET Image Estimation Using Local Linear Fitting. IEEE Transactions on Radiation and Plasma Medical Sciences, 2020, 4, 750-758.	2.7	1
35	Personalized iPSC-Derived Dopamine Progenitor Cells for Parkinson's Disease. New England Journal of Medicine, 2020, 382, 1926-1932.	13.9	298
36	ASCNET: Adaptive-Scale Convolutional Neural Networks for Multi-Scale Feature Learning. , 2020, , .		5

#	Article	IF	CITATIONS
37	Annotation-Free Gliomas Segmentation Based on a Few Labeled General Brain Tumor Images. , 2020, , .		1
38	AF-SEG: An Annotation-Free Approach for Image Segmentation by Self-Supervision and Generative Adversarial Network. , 2020, , .		4
39	Deep learning combined with radiomics may optimize the prediction in differentiating high-grade lung adenocarcinomas in ground glass opacity lesions on CT scans. European Journal of Radiology, 2020, 129, 109150.	1.2	24
40	Sparse Representation-Based Denoising for High-Resolution Brain Activation and Functional Connectivity Modeling: A Task fMRI Study. IEEE Access, 2020, 8, 36728-36740.	2.6	9
41	MRâ€based PET attenuation correction using a combined ultrashort echo time/multiâ€echo Dixon acquisition. Medical Physics, 2020, 47, 3064-3077.	1.6	12
42	Multi-label Detection and Classification of Red Blood Cells in Microscopic Images. , 2020, , .		6
43	Clinically Translatable Direct Patlak Reconstruction from Dynamic PET with Motion Correction Using Convolutional Neural Network. Lecture Notes in Computer Science, 2020, , 793-802.	1.0	3
44	Improved Patlak Reconstruction from Low-dose Dynamic PET Using Temporal Non-local Neural Network. , 2020, , .		0
45	IFGAN: Missing Value Imputation using Feature-specific Generative Adversarial Networks. , 2020, , .		4
46	Multi-Size Computer-Aided Diagnosis Of Positron Emission Tomography Images Using Graph Convolutional Networks. , 2019, , .		0
47	Gross tumor volume segmentation for head and neck cancer radiotherapy using deep dense multi-modality network. Physics in Medicine and Biology, 2019, 64, 205015.	1.6	79
48	PET image denoising using unsupervised deep learning. European Journal of Nuclear Medicine and Molecular Imaging, 2019, 46, 2780-2789.	3.3	157
49	Graph Convolutional Neural Networks For Alzheimer's Disease Classification. , 2019, 2019, 414-417.		55
50	Characteristics of Cognitive Deficit in Amnestic Mild Cognitive Impairment With Subthreshold Depression. Journal of Geriatric Psychiatry and Neurology, 2019, 32, 344-353.	1.2	14
51	Deep learning-enabled system for rapid pneumothorax screening on chest CT. European Journal of Radiology, 2019, 120, 108692.	1.2	34
52	Computationally efficient deep neural network for computed tomography image reconstruction. Medical Physics, 2019, 46, 4763-4776.	1.6	47
53	PET Image Deblurring and Super-Resolution With an MR-Based Joint Entropy Prior. IEEE Transactions on Computational Imaging, 2019, 5, 530-539.	2.6	27
54	A novel automatic hyper-parameter estimation for penalized PET reconstruction. , 2019, , .		0

#	Article	IF	CITATIONS
55	Predicting Alzheimer's Disease by Hierarchical Graph Convolution from Positron Emission Tomography Imaging. , 2019, , .		23
56	Low-dose dual energy CT image reconstruction using non-local deep image prior. , 2019, , .		7
57	Functional Neuroimaging in the New Era of Big Data. Genomics, Proteomics and Bioinformatics, 2019, 17, 393-401.	3.0	25
58	Iterative PET Image Reconstruction Using Convolutional Neural Network Representation. IEEE Transactions on Medical Imaging, 2019, 38, 675-685.	5.4	188
59	PET Image Reconstruction Using Deep Image Prior. IEEE Transactions on Medical Imaging, 2019, 38, 1655-1665.	5.4	172
60	Deep Learning-Based Image Segmentation on Multimodal Medical Imaging. IEEE Transactions on Radiation and Plasma Medical Sciences, 2019, 3, 162-169.	2.7	226
61	Time of flight PET reconstruction using nonuniform update for regional recovery uniformity. Medical Physics, 2019, 46, 649-664.	1.6	2
62	Early Diagnosis of Alzheimer's Disease Based on Resting-State Brain Networks and Deep Learning. IEEE/ACM Transactions on Computational Biology and Bioinformatics, 2019, 16, 244-257.	1.9	157
63	Consensus Neural Network for Medical Imaging Denoising with Only Noisy Training Samples. Lecture Notes in Computer Science, 2019, , 741-749.	1.0	32
64	CT-guided PET parametric image reconstruction using deep neural network without prior training data. , 2019, , .		11
65	EMnet: an unrolled deep neural network for PET image reconstruction. , 2019, , .		19
66	Population and individual information guided PET image denoising using deep neural network. , 2019, , .		3
67	Direct patlak reconstruction from dynamic PET using unsupervised deep learning. , 2019, , .		10
68	Artificial Intelligence and Machine Learning in Radiology: Opportunities, Challenges, Pitfalls, and Criteria for Success. Journal of the American College of Radiology, 2018, 15, 504-508.	0.9	445
69	Big data and medical research in China. BMJ: British Medical Journal, 2018, 360, j5910.	2.4	99
70	Decoding the orientation of contrast edges from MEG evoked and induced responses. NeuroImage, 2018, 180, 267-279.	2.1	40
71	P3â€090: JOINT DEBLURRING OF LONGITUDINAL DIFFERENTIAL PET IMAGES OF TAU. Alzheimer's and Dementia, 2018, 14, P1100.	0.4	0
72	ICâ€Pâ€203: JOINT DEBLURRING OF LONGITUDINAL DIFFERENTIAL PET IMAGES OF TAU. Alzheimer's and Dement 2018, 14, P167.	ia _{0.4}	0

#	Article	IF	CITATIONS
73	Neurogenetic contributions to amyloid beta and tau spreading in the human cortex. Nature Medicine, 2018, 24, 1910-1918.	15.2	135
74	Subject-specific brain tumor growth modelling via an efficient Bayesian inference framework. , 2018, 10574, .		2
75	Attenuation correction for brain PET imaging using deep neural network based on Dixon and ZTE MR images. Physics in Medicine and Biology, 2018, 63, 125011.	1.6	97
76	Penalized PET Reconstruction Using Deep Learning Prior and Local Linear Fitting. IEEE Transactions on Medical Imaging, 2018, 37, 1478-1487.	5.4	154
77	Cognitive Assessment Prediction in Alzheimer's Disease by Multi-Layer Multi-Target Regression. Neuroinformatics, 2018, 16, 285-294.	1.5	19
78	Medical image segmentation based on multi-modal convolutional neural network: Study on image fusion schemes. , 2018, , .		46
79	RBC Semantic Segmentation for Sickle Cell Disease Based on Deformable U-Net. Lecture Notes in Computer Science, 2018, , 695-702.	1.0	20
80	Joint estimation of activity image and attenuation sinogram using time-of-flight positron emission tomography data consistency condition filtering. Journal of Medical Imaging, 2017, 4, 023502.	0.8	5
81	Image deblurring using a joint entropy prior in x-ray luminescence computed tomography. Proceedings of SPIE, 2017, , .	0.8	0
82	Tau and amyloid Î ² proteins distinctively associate to functional network changes in the aging brain. Alzheimer's and Dementia, 2017, 13, 1261-1269.	0.4	90
83	Partial volume correction for PET quantification and its impact on brain network in Alzheimer's disease. Scientific Reports, 2017, 7, 13035.	1.6	37
84	Diagnostic Assessment of Deep Learning Algorithms for Detection of Lymph Node Metastases in Women With Breast Cancer. JAMA - Journal of the American Medical Association, 2017, 318, 2199.	3.8	2,003
85	Iterative Low-Dose CT Reconstruction With Priors Trained by Artificial Neural Network. IEEE Transactions on Medical Imaging, 2017, 36, 2479-2486.	5.4	175
86	Lowâ€dose CT reconstruction using spatially encoded nonlocal penalty. Medical Physics, 2017, 44, e376-e390.	1.6	23
87	Multi-Materials Decomposition using clinical Dualenergy CT. , 2017, , .		0
88	Penalized PET Reconstruction using CNN Prior. , 2017, , .		1
89	HOSVD-Based Multigraph Cuts for Joint Segmentation of Multi-Channel Images. , 2017, , .		0
90	A novel approach to assess the treatment response using Gaussian random field in PET. Medical Physics, 2016, 43, 833-842.	1.6	2

#	Article	IF	CITATIONS
91	Gold classification of COPDGene cohort based on deep learning. , 2016, , .		7
92	Clinical decision support for Alzheimer's disease based on deep learning and brain network. , 2016, , .		36
93	Localizing Sources of Brain Disease Progression with Network Diffusion Model. IEEE Journal on Selected Topics in Signal Processing, 2016, 10, 1214-1225.	7.3	30
94	Numerical observer for atherosclerotic plaque classification in spectral computed tomography. Journal of Medical Imaging, 2016, 3, 035501.	0.8	4
95	Dual-energy CT Reconstruction using Guided Image Filtering. , 2016, , .		0
96	Direct parametric imaging of reversible tracers using partial dynamic data. , 2016, , .		3
97	National Electrical Manufacturers Association and Clinical Evaluation of a Novel Brain PET/CT Scanner. Journal of Nuclear Medicine, 2016, 57, 646-652.	2.8	29
98	Matched signal detection on graphs: Theory and application to brain imaging data classification. NeuroImage, 2016, 125, 587-600.	2.1	34
99	Penalized direct estimation of parametric images in PET. , 2015, , .		3
100	Fast estimation of image variance for time-of-flight PET reconstruction. , 2015, , .		0
101	A Spectral Graph Regression Model for Learning Brain Connectivity of Alzheimer's Disease. PLoS ONE, 2015, 10, e0128136.	1.1	35
102	Sparse-View Spectral CT Reconstruction Using Spectral Patch-Based Low-Rank Penalty. IEEE Transactions on Medical Imaging, 2015, 34, 748-760.	5.4	124
103	Pulmonary imaging using respiratory motion compensated simultaneous PET/MR. Medical Physics, 2015, 42, 4227-4240.	1.6	26
104	Direct estimation from list-mode data for reversible tracers using graphical modeling. , 2015, , .		12
105	PET point spread function modeling and image deblurring using a PET/MRI joint entropy prior. , 2015, , .		7
106	4D numerical observer for lesion detection in respiratoryâ€gated PET. Medical Physics, 2014, 41, 102504.	1.6	3
107	¹⁸ F-Alfatide II and ¹⁸ F-FDG Dual-Tracer Dynamic PET for Parametric, Early Prediction of Tumor Response to Therapy. Journal of Nuclear Medicine, 2014, 55, 154-160.	2.8	43
108	Relative role of motion and PSF compensation in wholeâ€body oncologic PETâ€MR imaging. Medical Physics, 2014, 41, 042503.	1.6	35

#	Article	IF	CITATIONS
109	Patlak Image Estimation From Dual Time-Point List-Mode PET Data. IEEE Transactions on Medical Imaging, 2014, 33, 913-924.	5.4	54
110	Accuracy of respiratory motion compensated image reconstruction using 4DPET-derived deformation fields. , 2014, , .		0
111	A novel approach to the assessment of treatment response based on Gaussian random field. , 2014, , .		1
112	Respiratory motion compensation in simultaneous PET/MR using a maximum a posteriori approach. , 2013, , .		8
113	A graph theoretical regression model for brain connectivity learning of Alzheimer'S disease. , 2013, , .		18
114	Magnetic Resonance-Guided Positron Emission Tomography Image Reconstruction. Seminars in Nuclear Medicine, 2013, 43, 30-44.	2.5	92
115	Magnetic Resonance-Based Motion Correction for Positron Emission Tomography Imaging. Seminars in Nuclear Medicine, 2013, 43, 60-67.	2.5	89
116	Direct reconstruction of cardiac PET kinetic parametric images using a preconditioned conjugate gradient approach. Medical Physics, 2013, 40, 102501.	1.6	18
117	Treadmill exercise elevates striatal dopamine D2 receptor binding potential in patients with early Parkinson's disease. NeuroReport, 2013, 24, 509-514.	0.6	181
118	Non-Local Means Denoising of Dynamic PET Images. PLoS ONE, 2013, 8, e81390.	1.1	115
119	Quantitative Methods for Molecular Diagnostic and Therapeutic Imaging. Theranostics, 2013, 3, 729-730.	4.6	1
120	Quantitative Statistical Methods for Image Quality Assessment. Theranostics, 2013, 3, 741-756.	4.6	40
121	Spatially varying regularization for motion compensated PET reconstruction. , 2012, , .		4
122	Constrained mixture modeling for the estimation of kinetic parameters in dynamic PET. , 2012, , .		2
123	Dual-time-point Patlak estimation from list mode PET data. , 2012, , .		6
124	Dynamic PET and Optical Imaging and Compartment Modeling using a Dual-labeled Cyclic RGD Peptide Probe. Theranostics, 2012, 2, 746-756.	4.6	34
125	PET Image Reconstruction Using Information Theoretic Anatomical Priors. IEEE Transactions on Medical Imaging, 2011, 30, 537-549.	5.4	96
126	A nonlocal averaging technique for kinetic parameter estimation from dynamic PET data. , 2011, , .		1

8

#	Article	IF	CITATIONS
127	Exercise elevates dopamine D2 receptor in a mouse model of Parkinson's disease: In vivo imaging with [¹⁸ F]fallypride. Movement Disorders, 2010, 25, 2777-2784.	2.2	136
128	Sulcal set optimization for cortical surface registration. NeuroImage, 2010, 50, 950-959.	2.1	19
129	Iterative Image Reconstruction Using Inverse Fourier Rebinning for Fully 3-D PET. IEEE Transactions on Medical Imaging, 2007, 26, 745-756.	5.4	27
130	Statistical Modeling and Reconstruction of Randoms Precorrected PET Data. IEEE Transactions on Medical Imaging, 2006, 25, 1565-1572.	5.4	18